VNU Journal of Science: Mathematics - Physics
Journal homepage: https://js.vnu.edu.vn/MaP

Original Article

Enhanced Hard Magnetic Performance for MnBi Green Powders

Nguyen Hoai Nam[1], Vuong Kha Anh[1,2,3], Le Nguyen Nhut Tan[4], Pham Hong Nam[1], Vuong Thi Kim Oanh[1], Tran Bao Trung[1], Le Tuan Minh[1], Nguyen Van Toan[1], Dang Minh Triet[4], Nguyen Van Khanh[5], Nguyen Van Vuong[1], Nguyen Xuan Truong[1,2,*]

[1]*Institute of Materials Science, Vietnam Academy of Science and Technology 18 Hoang Quoc Viet, Cau Giay, Hanoi, Vietnam*

[2]*University of Science and Technology of Hanoi, Vietnam Academy of Science and Technology, 18 Hoang Quoc Viet, Cau Giay, Hanoi, Vietnam*

[3]*Hanoi Metropolitan University, 98 Duong Quang Ham, Cau Giay, Hanoi, Vietnam*

[4]*Can Tho University, 3/2 Road, Ninh Kieu, Can Tho, Vietnam*

[5]*Hanoi National University of Education, 136 Xuan Thuy, Cau Giay, Hanoi, Vietnam*

Received 26 September 2023
Revised 18 March 2024; Accepted 02 May 2024

Abstract: $Mn_{55}Bi_{45}$ melt - spun ribbons were prepared by using the melt-spinning technique followed by annealing in $Ar/5\%H_2$ gas mixture. The in-situ formation of ferromagnetic phase (denoted as LTP) of MnBi was observed by the multi-section cycled Differential Scanning Calorimetry (DSC) method. It was found that, the optimal annealing temperature range for forming MnBi LTP is 250 – 280 ^oC. The prolonging annealing time increases the content of MnBi LTP leading to the increase of saturation magnetization M_s but paid by the drop of the intrinsic coercivity ${}_iH_c$. The MnBi green powders were prepared by the Low Energy Ball Milling method (LEBM) in N_2 liquid. The maximum energy product of MnBi green powders is estimated about 10.8 MGOe.

Keywords: Melt-spun ribbons, microstructure, magnetic properties, saturation magnetization, MnBi green powders.

* Corresponding author.
E-mail address: truongnx@ims.vast.vn

https//doi.org/10.25073/2588-1124/vnumap.4880

1. Introduction

In the recent years, the demand of permanent magnets (worth $34,400 Million by 2021 [1]) has been increased because of growing their applications in electronics, renewable energy, automotive industries. However, the shortage in rare earth supply [2] and the crisis in price increase of Nd and Dy [3] cause difficulties in production of NdFeB-based permanent magnets. Therefore, the development of rare-earth-free permanent magnets becomes very important.

MnBi-based hard magnetic materials were investigated since the early 1950 s [4]. With the instrinsic characteristics of the moderate spontaneous magnetization (M_{sp}) of 8.2 kG, the high magneto-crystalline energy (K_a) of 0.9 MJ/m^3, the elevated Curie temperature (T_c) of 360 ^{o}C and especially the positive temperature coefficient of coercivity $d(_iH_c)/dT > 0$, the MnBi-based magnets become alternative of NdFeB-based magnets for high-temperature applications [5]. However, over past 60 years, instead of the numerous spent efforts, the quality of MnBi-based magnets is restricted by the moderate value of maximum energy product $(BH)_{max}$ of 8.4 MGOe [6] that is far below the theoretical limit of 17.6 MGOe [7].

In fact, as shown on the phase diagram (see Fig. 1b), the MnBi alloy can be formed in two phases, one of that is responsible for ferromagnetism and formed at the temperature lower than 340 ^{o}C with the hexagonal crystal structure, the another is paramagnetic and formed at higher temperature of 365 ^{o}C with the orthorhombic structure. According to the formation temperatures, these two phases are noted as LTP (Low Temperature Phase) for the first phase and HTP (High Temperature Phase) for the second one. Because of the complex phase diagram of Mn-Bi system, the MnBi alloys are peritectically solidified forming the multi-phase alloys that requires the followed annealing process to enhance the LTP content. Moreover, the initial composition of weighted Mn and Bi amounts effects on the formation of LTP as shown by Cui et al., [8]. Their results indicated that, to maximize the LTP content, the weighed Mn-rich composition of $Mn_{55}Bi_{45}$ should be preferred that was used in this work.

Up to now, the MnBi powder with high LTP content and coercivity is prepared by melt-spinning MnBi alloy into ribbons followed by pulverizing obtained ribbons in a protection gas atmosphere [9-16]. This powder is called as the green powder since it is utilized as a starting powder used for magnet compaction process. It is worthy to note that the large difference in the melting temperature (T_m) of Mn and Bi and the strong reactivity of Bi with the copper wheel of spinner make the formation of high-performance MnBi ribbons very difficult. Meanwhile, the challenge in producing of MnBi high-performance magnets requires the remanence magnetization M_r balanced with the remanence coercivity $_BH_c$ kept around of 6 ÷ 7 kOe.

In this work, we present our efforts to prepare melt-spun high-performance MnBi LTP ribbons and high-performance MnBi green powders for use in a large-scale manufacturing of MnBi high-performance bulk magnets. All the technological parameters will be discussed in details.

2. Experimental

The alloys with nominal compositions of $Mn_{55}Bi_{45}$ were arc-melted from the starting high-purity metals (Mn and Bi, 99.95%) under argon atmosphere. The ingots were melted three times to ensure their homogeneity. 10g per batch of this pre-alloys was remelted in the high-quality quartz tube of a commercial melt-spinner and ejected onto a rotating copper wheel lubricated with a thin layer of graphene oil in 0.05 MPa argon atmosphere. The wheel speeds were regulated in the range from 5 to 35 m/s, the quartz tube orifice diameter was fixed at 0.8 mm, the distance between the nozzle and the wheel surface was kept constant by 3 mm. The prepared melt-spun ribbons were annealed at 280 ± 5 ^{o}C in Ar/5%H_2 gas mixture for different times ranging up to 15 h. For preparing MnBi green powders, the

annealed MnBi ribbons were milled in N_2 liquid by low-energy ball milling method (LEBM). The composition phases of as-spun ribbons and annealed ones were characterized by D8 advance Brucker X-ray diffractometer (XRD) with Cu-Kα radiation with the scattering 2θ angle scan in the range from 25 to 75 degrees by the scanning step of 0.05° for the hold time of 3 s. The thermodynamic behavior of materials was analyzed by DSC trace method on Labsys Evo system at a chosen heating profile in a pure argon flow. The morphology of ribbon was studied by Hitachi-S4800 field emission scanning electron microscopy (FESEM). The hysteresis loops of prepared MnBi ribbons were measured by the Pulse Field Magnetometer (PFM).

3. Results and Discussion

Fig. 1a plots the XRD patterns of MnBi ribbons melt-spun at different wheel speeds. All peaks belong to the phases of MnBi, Bi and Mn. The ratio of these peak intensities versus wheel velocities reflects the complexity of rapid quench process of MnBi system. Depending on the phase diagram shown in Fig. 1b, one recognizes the peritectic solidification of the Mn-Bi system leading to the multi-phase microstructure of ribbons consisting of Bi and Mn phases. The LTP phase appeared in this multi-phase microstructure is caused by the combination between Mn and Bi grains. Because this combination follows the time-dependent diffusion mechanism with the low diffusion coefficient D ~ 10^{-12} cm^2/s [17] and the MnBi LTP is formed only at T ≤ 340 °C, the MnBi LTP content is low and depends on the wheel speed used. The lower spinning speed is, the higher MnBi LTP content achieves. Particularly, at v = 5 m/s the MnBi LTP content is estimated of 38 %wt. using the method presented in [18].

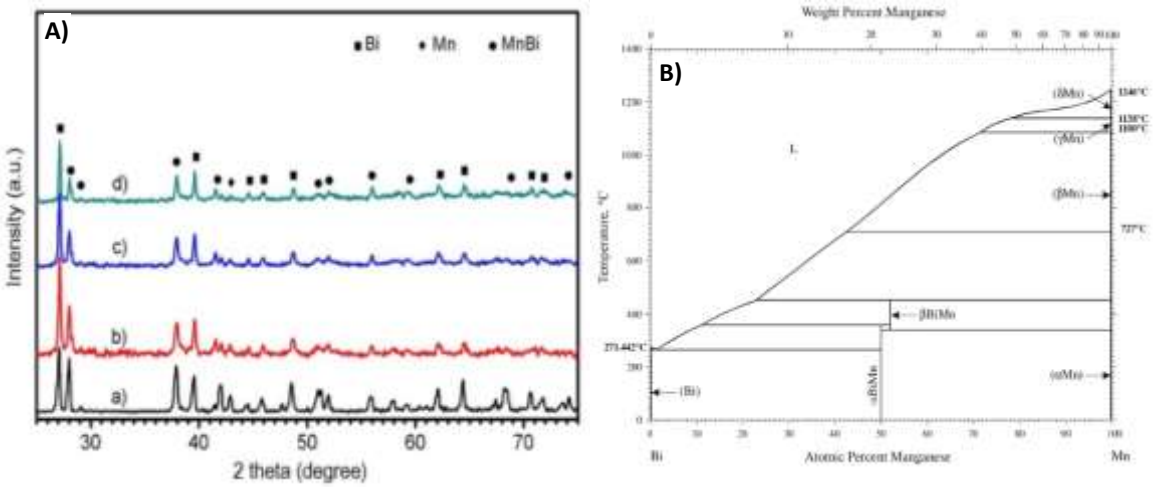

Figure 1. A) XRD patterns of MnBi ribbons melt-spun at: a) v = 5 m/s; b) v = 15 m/s; c) v = 25 m/s; d) v = 35 m/s. B) The phase diagram of Mn-Bi system [19].

The magnetic properties of these as-spun ribbons were checked by measuring the room temperature magnetization loops on the PFM with the maximal magnetized magnetic field H_{max} = 40 kOe. The loops plotted in Fig. 2 show the decrease of M_s of ribbons from 35 to 10 emu/g when the wheel speed increases from 5 to 35 m/s. This decrease corresponds to the above-mentioned descent of MnBi LTP content. In contrast, by increasing wheel speed, the coercivity of the as-spun ribbons is

increased from 3.7 to 5.9 kOe. This result is conventional and corresponds to the reduction of the MnBi particle sizes caused by increasing the cooling rate of ribbons.

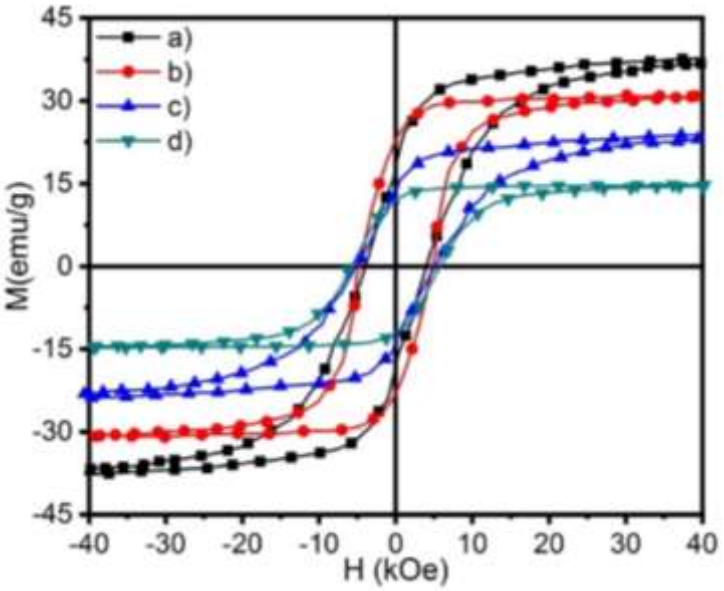

Figure 2. M(H) loops of MnBi ribbons melt-spun at: a) v = 5m/s; b) v = 15 m/s; c) v = 25 m/s; d) v = 35 m/s.

It is known, that MnBi LTP is formed by the diffusive combination of Mn and Bi [17], so this combination should be completed fast if the sizes of Mn and Bi grains are small. This conclusion pushes using the MnBi ribbons melt-spun at high cooling rate with the wheel speed v = 35 m/s followed by the elongated anneal at around 280 ^{o}C to increase further the MnBi LTP content of ribbons.

Fig. 3 shows the thickness and the cross-section morphologies of the ribbon melt-spun at v = 35 m/s. The ribbon is fairly uniform, the thickness is around 33 μm and the grain size is in the range of 50 ÷ 200 nm.

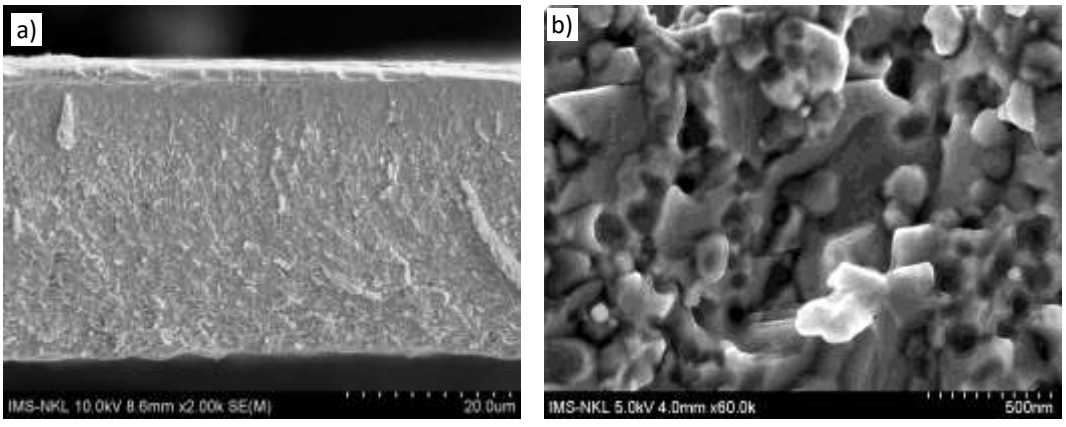

Figure 3. FESEM images of MnBi ribbons melt-spun with v = 35 m/s: a) the ribbon thickness; b) the ribbon particles morphology.

To investigate the evolution of the MnBi LTP formation, the multi-sectioned DSC trace of MnBi ribbons melt-spun at v = 35 m/s was recorded and shown in Fig. 4. The first endothermic peak located at 263 – 265 °C is the peak of the melting state of the eutectic composition $Bi_{98}Mn_2$ [20]. The exothermic peak at 251 – 255 °C principally corresponds to the crystallization of the MnBi LTP [20]. By keeping the sample in the temperature range of 200 ÷ 280 °C for 5 cycles, the LTP content inside the ribbon is gained continuously. During each cycle, the MnBi LTP content is formed resulting in decrease of free Bi and Mn. The high content of MnBi LTP is proved by the huge endothermic peak located at 350 °C revealing the energy change occurred at the Curie temperature of MnBi LTP, where the transition from the ferromagnetic state to paramagnetic state is occurred.

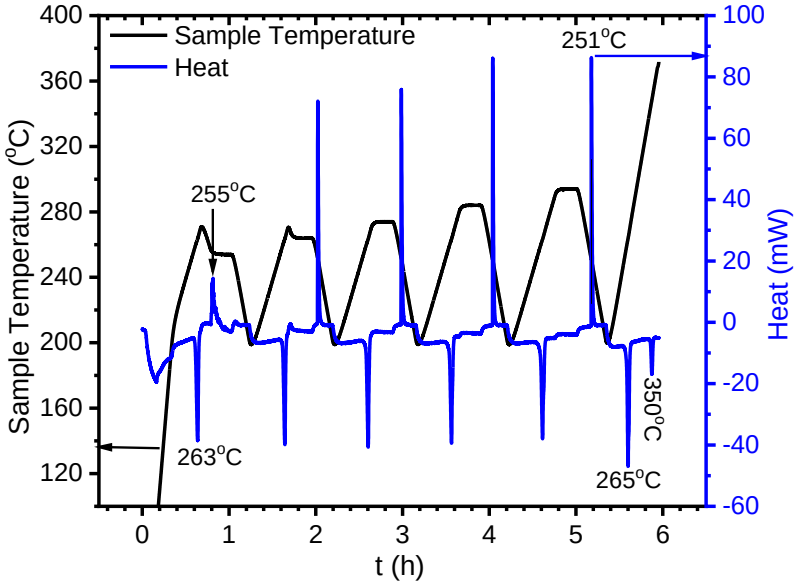

Figure 4. The multi-sectioned DSC trace of the MnBi ribbon melt-spun at v = 35 m/s.

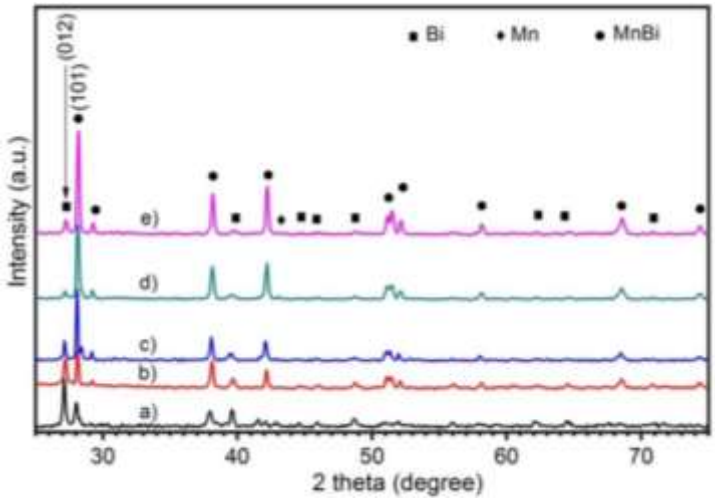

Figure 5. The XRD patterns of MnBi ribbon melt-spun at v = 35 m/s and annealed at 280 °C for a) 0 h; b) 3 h; c) 9 h, d) 12 h and e) 15 h.

On the basics of the mentioned MnBi LTP evolution, the MnBi ribbon melt-spun at v = 35 m/s were annealed in the tube furnace at 280 ^{o}C in Ar/5%H2 gas mixture for 3, 6, 9, 12 and 15 h. The XRD patterns plotted in Fig. 5 show the time-dependent increase of the intensity of the main diffraction peaks of MnBi located at 28.14 degree. By increasing the annealing time, the intensity ratio between the strongest peaks of MnBi and Bi (IMnBi(101)/IBi(012)) increased. Moreover, the peak (101) of MnBi becomes sharper indicating that the grains grown up during the annealing process. As a consequence of this MnBi LTP formation, the strongest peak of the Mn phase located at $2\theta = 43.02^{o}$ is not observed after 9h of heat treatment. The MnBi LTP content reached the value of 95 wt.% after 12 h annealing. The MnBi LTP content is unchanged after annealing for 15 h.

The M_s and $_iH_c$ values of the hand and LEBM-milled (for 120 min.) MnBi powders versus their annealing time ranging from 0 to 15 h were summarized in Fig 6. The coercivity $_iH_c$ obviously drops from 5.9 to 2.1 kOe after 15h annealing. Meanwhile, the saturation magnetization M_s of ribbons was increased from 10 emu/g to 70 emu/g after 12 h annealing. This high value of 70 emu/g is compared to the recent works [21, 22].

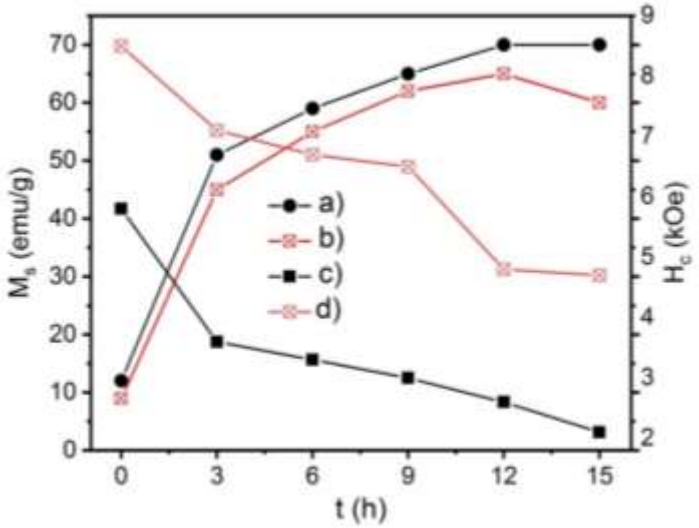

Figure 6. The magnetic properties versus the annealing times: a) M_s, c) H_c of hand milling MnBi powders; and b) M_s, d) $_iH_c$ of LEBM MnBi powders for 120 minutes.

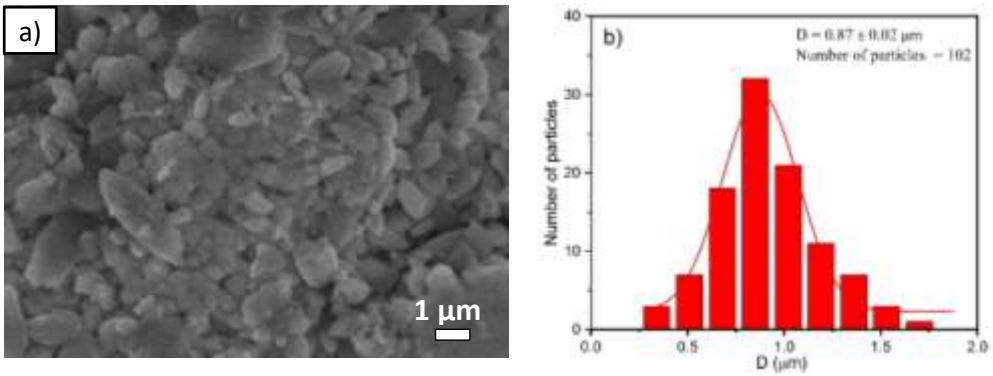

Figure 7. The morphology of LEBM MnBi powders (a) and particles distribution (b) of MnBi powders LEB milled for 120 minutes.

According to the relation between the size of Mn and Bi grains and the annealing time t_a described in [17], to optimize the annealing time t_a. The melt-spun ribbons were annealed at 280 ^oC for 9 h, which were ground for 120 min. to get the grain size and the grain size distribution as shown in Fig. 7. The mean diameter of grains is 0.87 μm, meanwhile the single domain size of MnBi about 0.5 μm.

Finanly, these obtained MnBi green powders are aligned in the epoxy resin diluted by using xylene under 18 kG magnetic field to form the in-epoxy bonded rectangular magnet sample with the length to edges ratio large enough to skip the effect of the demagnetization field. The magnetic characteristics of these aligned MnBi green powders were estimated with the density of 8.9 g/cm^3 and presented in the Fig. 8. The obtained results include $_iH_c$ = 14.8 kOe, $_bH_c$ = 6.5 kOe, M_r = 6.7 kG and $(BH)_{max}$ = 10.8 MGOe.

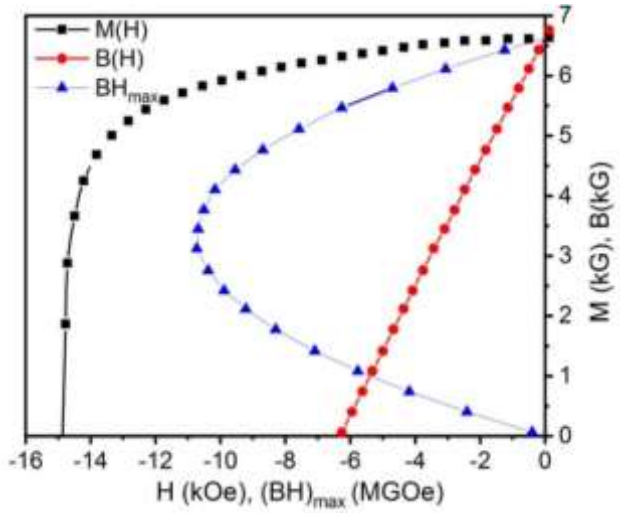

Figure 8. The M(H), B(H) and $(BH)_{max}$ curves of LEB milled and annealed MnBi powders bonded in the diluted epoxy resin under 18 kG aligning magnetic field.

4. Conclusion

The MnBi LTP ribbons were fabricated by means of the melt-spinning technique using the conventional commercial rapid quench furnace ZGK-1 followed by the subsequent annealing at 280 ^oC. The in-situ multi-sectioned DSC trace revealed the intensive growth of the ferromagnetic phase at 251 - 255 ^oC. The coercivity $_iH_c$ of MnBi ribbons melt-spun at v = 35 m/s measured at 40 kOe is 5.9 kOe. The MnBi ribbons with the highest MnBi LTP content of 95 wt.% and M_s of 70 emu/g were obtained by 12 h annealing at 280 ^oC. The high-performance green MnBi powders have been prepared from the MnBi ribbons melt-spun at 35 m/s, annealed at 280 ^oC for 9 h, and LEB milled for 120 min. The energy product of this green powder achieves 10.8 MGOe that is high enough for making MnBi high-performance bulk magnets in the mass scale.

Acknowledgement

We gratefully acknowledge financial support from the Ministry of Science and Technology (MOST) under project NĐT/CN/21/25.

References

[1] Permanent Magnet Market, By Types (NdFeB, Ferrite, SmCo), End User Industry (Consumer Electronics, General Industrial, Automotive, Medical Technology, Environment & Energy) and Region - Global Forecast to 2026, https://www.marketsandmarkets.com/Market-Reports/permanent-magnet-market-806.html (accessed on: September 2nd, 2023).

[2] O. Gutfleisch, M. A. Willard, E. Bruck, C. H. Chen, S. G. Sankar, J. P. Liu, Magnetic Materials and Devices for the 21st Century: Stronger, Lighter, and More Energy Efficient, Advanced Materials, Vol. 23, 2011, pp. 821-842, https://doi.org/10.1002/adma.201002180.

[3] D. Kaihong, The Rare Earth Magnet Industry and Rare Earth Price in China, EPJ Web of Conferences, Vol. 75, 2014, 0400 5 (3 pages), https://doi.org/10.1051/epjconf/20147504005.

[4] E. Adams, W. M. Hubbard, A. M. Syeles, A New Permanent Magnet from Powdered Manganese Bismuthide, Journal Applied Physics, Vol. 23, 1952, pp.1207-1211, https://doi.org/10.1063/1.1702032.

[5] J. M. D. Coey, New Permanent Magnets; Manganese Compounds, Journal of Physics: Condensed Matter, Vol. 26, No. 6, 2014, 064211 (6 pages), https://doi.org/10.1088/0953-8984/26/6/064211.

[6] V. V. Nguyen, N. Poudyal, X. Liu, J. P. Liu, K. Sun, M. J. Kramer, J. Cui, High-Performance MnBi Alloy Prepared Using Profiled Heat Treatment, IEEE Transactions on Magnetics, Vol. 50, No. 12, 2014, pp 1-6, https://doi.org/10.1109/TMAG.2014.2341659.

[7] J. Cui, J. P. Choi, G. Li, E. Polikarpov, J. Darsell, N. Overman, M. Olszta, D. Schreiber, M. Bowden, T. Droubay, M. J. Kramer, N. A. Zarkevich, L. L. Wang, D. D. Johnson, M. Marinescu, I. Takeuchi, Q. Z. Huang, H. Wu, H. Reeve, N. V. Vuong, J. P. Liu, Thermal Stability of MnBi Magnetic Materials, Journal of Physics: Condensed Matter, Vol. 26, No. 6, 2014, 064212 (10 pages), https://doi.org/10.1088/0953-8984/26/6/064212.

[8] J. Cui, J. P. Choi, E. Polikarpov, M. E. Bowden, W. Xie, G. Li, Z. Nie, N. Zarkevich, M. J. Kramer, D. Johnson, Effect of Composition and Heat Treatment on MnBi Magnetic Materials, Acta Materialia, Vol. 79, 2014, pp. 374-381, https://doi.org/10.1016/j.actamat.2014.07.034.

[9] C. S. Lakshmi, R. W. Smith, Structural and Magnetic Propertiesof Rapidly Quenched Bi-Mn Alloys, Materials Science and Engineering: A, Vol. 133, 1991, pp. 241-244, https://doi.org/10.1016/0921-5093(91)90060-Z.

[10] X. Guo, Z. Altounian, J. O. S. Olsen, Formation of MnBi Ferromagnetic Phases Through Crystallization of the Amorphous Phase, Journal of Applied Physics, Vol. 69, 1991, pp. 6067-6069, https://doi.org/10.1063/1.347771.

[11] K. Kang, L. H. Lewis, A. R. Moodenbaugh, Crystal Structure and Magnetic Properties of MnBi–Bi Nanocomposite, Journal of Applied Physics, Vol. 97, 2005, 10K302 (3 pages), https://doi.org/10.1063/1.1847058.

[12] X. Guo, X. Chen, Z. Altounian, J. O. S. Olsen, Magnetic Properties of MnBi Prepared By Rapid Solidification, Physical Review B, Vol. 46, No. 22, 1992, pp. 14578-14582, https://doi.org/10.1103/PhysRevB.46.14578.

[13] Y. B. Yang, X. G. Chen, S. Guo, A. R. Yan, Q. Z. Huang, M. M. Wu, D. F. Chen, Y. C. Yang, J. B. Yang, Temperature Dependences of Structure and Coercivity for Melt-spun MnBi Compound, Journal of Magnetism and Magnetic Materials, Vol. 330, 2013, pp. 106-110, https://doi.org/10.1016/j.jmmm.2012.10.046.

[14] D. T. Zhang, W. T. Geng, M. Yue, W. Q. Liu, J. X. Zhang, J. A. Sundararajan, Y. Qiang, Journal of Magnetism and Magnetic Materials, Crystal Structure and Magnetic Properties of Mn_xBi_{100-x} (x=48, 50, 55 and 60) Compounds, Vol. 324, No. 11, 2012, pp. 1887-1890, https://doi.org/10.1016/j.jmmm.2012.01.017.

[15] S. Tetsuji, N. Ryuji, N. H. Daisuke, Magnetic Properties of Mn–Bi Melt-Spun Ribbons, Journal of Magnetism and Magnetic Materials, Vol. 349, 2014, pp. 9-14, https://doi.org/10.1016/j.jmmm.2013.08.031.

[16] P. Kharel, V. R. Shah, R. Skomski, J. E. Shield, D. J. Sellmyer, Magnetism of MnBi-Based Nanomaterials, IEEE Transactions on Magnetics, Vol. 49, No. 7, 2013, pp. 3318-3321, https://doi.org/10.1109/TMAG.2013.2245497.

[17] N. V. Vuong, N. X. Truong, Low Temperature Phase of the Rare-earth-free MnBi Magnetic Material, Journal of Science and Technology, Vol. 54, No. 1A, 2016, pp. 50-57, https://doi.org/10.15625/2525-2518/54/1A/11805.

[18] N. X. Truong, N. V. Vuong, Preparation and Magnetic Properties of MnBi Alloy and its Hybridization with NdFeB, Journal of Magnetics, Vol. 20, No. 4, 2015, pp. 336-341, https://doi.org/10.4283/JMAG.2015.20.4.336.

[19] H. Okamoto, Supplemental Literature Review of Binary Phase Diagrams: Ag-Co, Ag-Er, Ag-Pd, B-Ce, Bi-La, Bi-Mn, Cu-Ge, Cu-Tm, Er-Y, Gd-Tl, H-La, and Hg-Te, Journal of Phase Equilibria and Diffusion, Vol. 36, 2015, pp. 10-21, https://doi.org/10.1007/s11669-014-0341-7.

[20] X. Guo, A. Zaluska, Z. Altounian, J. O. S. Olsen, The Formation of Single-Phase Equiatomic Mnbi by Rapid Solidification, Journal of Materials Research, Vol. 5, 1990, pp. 2646-2651, https://doi.org/10.1557/JMR.1990.2646.

[21] Y. Yang, J. T. Lim, J. Park, N. K. Kim, H. D. Qian, O. L. Li, J. W. Kim, C. J. Choi, Effects of Sn Addition on the Microstructure and Magnetic Properties of MnBi Bulk Magnets, Journal of Alloys and Compounds, Vol. 891, 2022, pp. 161999, https://doi.org/10.1016/j.jallcom.2021.161999.

[22] S. Lu, S. Shuai, L. Chen, Z. Xiang, W. Lu, Effect of Mg Content on the Microstructure and Magnetic Properties of Rare-earth-free MnBi Alloys, Journal of Magnetism and Magnetic Materials, Vol. 570, 2023, pp. 170499, https://doi.org/10.1016/j.jmmm.2023.170499.